

Targeting Cells That Overexpress the Epidermal Growth Factor Receptor with Polyethylene Glycolated BPD Verteporfin Photosensitizer Immunoconjugates[¶]

Mark D. Savellano^{1,2} and Tayyaba Hasan^{*3}

¹Department of Surgery, Dartmouth-Hitchcock Medical Center, Lebanon, NH;

²Thayer School of Engineering, Dartmouth College, Hanover, NH and

³Wellman Laboratories of Photomedicine, Department of Dermatology, Harvard Medical School, Massachusetts General Hospital, Boston, MA

Received 3 January 2003; accepted 17 January 2003

ABSTRACT

Photoimmunotherapy was introduced two decades ago but has been studied infrequently *in vivo* and is virtually untested clinically. Progress has been limited because high-quality, well-characterized photosensitizer immunoconjugates (PICs) have been difficult to make. Here, we describe the development of an innovative conjugation method for producing water-soluble PICs that are free of insoluble aggregates and free of unacceptable amounts of noncovalently associated photosensitizer impurities. The method exploits two procedures previously untried in this research area. First, a small number of antibody lysines (<3 per antibody) are polyethylene glycolated (PEGylated) using a 10 kDa branched polyethylene glycol (PEG), which dramatically enhances PIC solubility and reduces PIC aggregation. Second, a 50% dimethyl sulfoxide–50% aqueous two-solvent system is used to prevent photosensitizer aggregation and noncovalent interactions. These measures allow efficient covalent linkage of the photosensitizer BPD Verteporfin (BPD) to antibody lysines, thorough purification of the resulting PICs (verified by sodium dodecyl sulfate–polyacrylamide gel electrophoresis), maintenance of PIC antigen-binding activity (verified by cellular binding–uptake assays) and reduction of nonspecific cellular uptake (*e.g.* macrophage capture) of the PICs. Loading levels could be

varied controllably in the range ≤ 11 BPD/antibody. PICs of the C225 anti–epidermal growth factor receptor (EGFR) chimeric monoclonal antibody killed EGFR-overexpressing A-431 cells photodynamically but did not significantly affect EGFR-negative NR6 cells. Although fluorescence measurements demonstrated that the PICs were quenched by as much as an order of magnitude compared with free BPD, an impressive 90% reduction in A-431 cell viability was achieved using 20 J/cm² of 690 nm light after a 40 h incubation with the C225 PICs. The results suggest that PEGylated BPD-C225 PICs merit further investigation in animal models of EGFR-overexpressing cancers.

INTRODUCTION

Photoimmunotherapy (PIT), which uses photosensitizer immunoconjugates (PICs) to improve the specificity of photosensitizer delivery, could broaden the applicability of photodynamic therapy (PDT). For example, it has been suggested that PDT might be used effectively in the treatment of small diffuse malignancies present in a cavity such as the peritoneum or bladder if the photosensitizer can be made to accumulate with high specificity in malignant cells (1). This would allow photodynamic destruction of diseased cells while sparing adjacent normal tissues of sensitive organs. Previously, dose-limiting toxic effects, including small-bowel complications, pleural effusions and gastric perforation, were noted in a Phase-I trial for PDT of intraperitoneal tumors using the small-molecule photosensitizer preparation Photofrin[®] (2). In an effort to alleviate these problems, PIT is being investigated because it offers the possibility of targeting intraperitoneal tumors much more specifically than does conventional PDT (3).

Although nearly 20 years have passed since the first report of PIT (4), no clinically beneficial PIC yet exists. Literature reviews of PIC research (5–8) have concluded that a major impasse encountered in this field has been the synthesis and purification of functional, well-characterized conjugates. Understandably, the poor characterization of PIC preparations used in earlier studies has made it difficult to ascertain what improvements might be made to generate conjugates of clinical utility. In particular, many previous studies of PICs did not rigorously address the question of whether the photodynamic effects of the conjugate preparations were due to the specific action of the conjugates or to the action of

[¶]Posted on the website on 8 February 2003.

*To whom correspondence should be addressed at: Wellman Laboratories of Photomedicine, Department of Dermatology, Harvard Medical School, Massachusetts General Hospital, 314A Bartlett Building, 40 Blossom St., Boston, MA 02114, USA. Fax: 617-726-8566; e-mail: thasan@partners.org

Abbreviations: BPD, BPD Verteporfin, also referred to previously as benzoporphyrin derivative monoacid ring A or BPDMA; BPD–Ab, BPD–antibody; DMEM, Dulbecco modified Eagle medium; DMSO, dimethyl sulfoxide; DPBS, Dulbecco's phosphate-buffered solution; EDC, 1-ethyl-3-(3-dimethylaminopropyl) carbodiimide HCl; EGFR, epidermal growth factor receptor; IRF, instrument response function; Mab, monoclonal antibody; NHS, *N*-hydroxysuccinimide; PBS, phosphate-buffered saline without Ca and Mg; PDT, photodynamic therapy; PEG, polyethylene glycol; PEGylated, polyethylene glycolated; PIC, photosensitizer immunoconjugate; PIT, photoimmunotherapy; RbIgG, rabbit IgG; SDS-PAGE, sodium dodecyl sulfate–polyacrylamide gel electrophoresis.

© 2003 American Society for Photobiology 0031-8655/01 \$5.00+0.00

noncovalently associated photosensitizer impurities (5,6,8). This has been one of the more cumbersome issues encountered not only in PIC investigations but also in photosensitizer bioconjugate studies in general. Most photosensitizers used in PDT are hydrophobic, highly adsorptive and tend to aggregate in aqueous solutions, which has severely complicated the conjugation of photosensitizers to water-soluble macromolecules such as antibodies and has also made it difficult to remove noncovalently associated photosensitizer impurities from PIC preparations. For similar reasons, it has been difficult to prevent aggregation and maintain solubility of PIC preparations.

The aim of this study was to produce high-purity, soluble, well-characterized PICs and to test them for their specific phototoxicity against target cells. To this end, we chose to use well-characterized components for the construction of our PICs. The photosensitizer, BPD Verteporfin (BPD), has been thoroughly characterized (9,10), and it has been found to be a highly potent photosensitizer for PDT. Its toxicologic profile is well established, and it is approved for human use (11). The targeting antibody, C225, a chimeric antibody to the extracellular domain of the epidermal growth factor receptor (EGFR), has shown promise in the treatment of many cancers, either administered alone or in combination with radiation or chemotherapy (12–15). C225 is in Phase-I to Phase-III trials for a variety of cancers (16–18), and although it did not receive the approval of the Food and Drug Administration initially, its approval may still be anticipated in the future. It blocks autocrine activation of the EGFR by EGF and transforming growth factor- α , a process that is important for tumor cell proliferation. Moreover, the EGFR appears to be an excellent target for antibody-based cancer therapies given that it is overexpressed on the surface of roughly one third of all epithelial tumors (19,20).

The use of BPD in PIC investigations has already been extensively reported in the literature (21–25). However, like other PIC studies (26), these previous studies of BPD-based conjugates used impure PICs and did not demonstrate that the photodynamic activity of the PIC preparations was predominantly due to the activity of the conjugates and not due to the activity of noncovalently associated photosensitizer impurities. Furthermore, the conjugation protocols described in the literature for linking BPD directly to antibodies produced conjugate preparations that contained significant amounts of insoluble aggregates. This study describes our approach to solving these problems with the goal of generating high-purity, target-specific PICs using a monoclonal antibody (Mab) directed to the EGFR. We also demonstrate that these PICs photodynamically kill tumor cells that overexpress the EGFR *via* specific binding to this receptor.

MATERIALS AND METHODS

Cell lines and antibodies. A-431 human epidermoid carcinoma cells and J774A.1 (J774) mouse monocyte-macrophage cells were purchased from American Type Culture Collection (ATCC CRL-1555 and ATCC TIB-67, respectively; Rockville, MD). EGFR-negative variant 3T3-NR6 (NR6) cells, derived from the 3T3-Swiss albino embryonic mouse fibroblast cell line (27), were a generous gift from Dr. A. Wells (Department of Pathology, University of Alabama, Birmingham, AL). J774 cells were grown in Roswell Park Memorial Institute 1640 medium containing 10% heat-inactivated fetal bovine serum. A-431 cells were grown in Dulbecco modified Eagle medium (DMEM) containing 4.5 g/L glucose and 10% heat-inactivated fetal bovine serum. NR6 cells were grown in DMEM containing 1.0 g/L glucose and 10% heat-inactivated fetal bovine serum. All cell growth media were supplemented with 100 units/mL penicillin and 100 μ g/mL streptomycin. Cells were maintained in an incubator at 37°C in an atmosphere of 5% carbon dioxide.

C225 anti-EGFR chimeric Mab was a generous gift from ImClone Systems Incorporated (Somerville, NJ). Rabbit IgG (RbIgG) was obtained from Sigma-Aldrich (St. Louis, MO). Antibodies were prepared as 10 mg/mL stock solutions in phosphate-buffered saline (PBS; essentially, Dulbecco's phosphate-buffered solution [DPBS] without Ca and Mg), pH 7.4. C225 antibody, supplied as a 2 mg/mL stock solution was concentrated to 10 mg/mL and exchanged to PBS using a 50 kDa MW cut-off Centricon centrifugal filter device (Centricon YM-50, Millipore Corp., Bedford, MA). RbIgG, supplied as a lyophilized powder, was simply dissolved in PBS to 10 mg/mL.

Preparation of activated BPD-N-hydroxysuccinimide ester. BPD was a generous gift from QLT PhotoTherapeutics Incorporated (Vancouver, BC, Canada). The activated *N*-hydroxysuccinimide (NHS) ester of BPD was synthesized in dimethyl sulfoxide (DMSO) by mixing six volumes of 5 mg/ml BPD in its free monoacid form (6.96 mM) with five volumes of freshly prepared 5 mg/mL NHS (43.4 mM) and five volumes of freshly prepared 5 mg/mL 1-ethyl-3-(3-dimethylaminopropyl) carbodiimide HCl (EDC; 26.1 mM). To obtain the BPD-NHS ester in high yield without generating significant amounts of undesirable side products (28,29), the reaction was maintained at 4°C for at least 10 days. After the extended reaction period, the mixture was dried down and washed and extracted with water and methylene chloride three times. The extracted crude BPD-NHS product was then purified by silica gel chromatography with ethyl acetate as the eluant and methylene chloride as the loading solvent. Ethyl acetate was evaporated from the recovered product, and the purified BPD-NHS was then reconstituted in DMSO at roughly 2.5 mM concentration, as verified by absorbance measurement. (The extinction coefficient of BPD in DMSO is about 36 500 $M^{-1}\cdot\text{cm}^{-1}$ at 690 nm. It was assumed that BPD and BPD-NHS have similar absorption characteristics in this solvent at this wavelength.) Purified BPD-NHS was stored at or below -20°C until it was needed for the conjugation reaction.

Preparation of polyethylene-glycolated BPD PICs. Conjugations were conducted in a 50% DMSO–50% aqueous two-solvent system at room temperature. During mixing of the various reactants, care was taken to avoid exposing the antibody to greater than 50% DMSO content to prevent protein denaturation or precipitation. First, antibody was conjugated with a 10 kDa two-branched polyethylene glycol (PEG)-NHS ester (Shearwater Polymers, Huntsville, AL) by reacting 400 μ g of antibody (equivalent to 40 μ L of a 10 mg/mL stock in PBS) with either 54 or 108 μ g of the PEG-NHS ester (equivalent to 2 or 4 μ L of a 27 mg/mL stock in DMSO; stored at -20°C until needed) in a total volume of approximately 290 μ L. The PEG-NHS-antibody molar ratios were approximately 2 to 4. After a 1.5 h reaction period, varying amounts of the BPD-NHS were added to the reaction mixture, ranging from 2 to 30 μ L of the 2.5 mM BPD-NHS ester stock solution. The reaction was then allowed to proceed for another 2 h.

After a total reaction period of 3.5 h, the conjugation reaction mixture was centrifuged at 16 000 *g* for 5 min to remove any insoluble material. The crude PIC preparation was then purified on a 3 ml Sephadex G-50 (medium particle size; Amersham Pharmacia Biotech Inc., Piscataway, NJ) spun column (30), equilibrated in 50% DMSO–50% deionized–distilled H₂O. At this stage the purified PIC could be stored in 50% DMSO at 4°C. Under these storage conditions the PIC preparations remained stable at least for several months. Before use in cell culture experiments, the PIC preparations were usually diluted with PBS to decrease the DMSO content to roughly 5%, and then they were concentrated and exchanged to a purely aqueous PBS solution using a 50 kDa MW cut-off Centricon centrifugal filter device. Polyethylene-glycolated (PEGylated) PIC preparations that had been exchanged to purely aqueous PBS were stored at 4°C and remained stable at least for several months. When necessary, the PIC preparations were sterile filtered using a 0.2 μ m filter membrane. In some cases a small amount of albumin was added to the preparations before filtering to prevent any adsorption of the PIC to the filter membrane.

Estimation of the BPD-antibody molar loading ratios of the PICs. Ground state absorption spectra were measured using an HP 8453 UV-visible spectrophotometer (Hewlett Packard GmbH, Waldbronn, Germany). The ~690 nm absorbance peak of the PIC was compared with the ~690 nm absorbance peak of free-BPD standards in 50% DMSO–50% aqueous solutions to estimate the BPD content of the PIC. The protein content of the PIC was then measured by a Bradford-type protein assay (Bio-Rad Laboratories, Hercules, CA). Subsequently, a simpler method for estimating PIC-loading ratios was used, which yielded comparable results. In this second method the protein content of the PIC was instead estimated by subtracting the BPD contribution to the PIC absorbance at 280 nm. This approximate measure of the protein contribution to the PIC absorbance could then be compared with the 280 nm absorbance of unmodified antibody standard samples.

Sodium dodecyl sulfate–polyacrylamide gel electrophoresis analysis of the PICs. The PICs were analyzed using a sodium dodecyl sulfate (SDS)–discontinuous buffer polyacrylamide gel electrophoresis (PAGE) system (Mini-PROTEAN II cell electrophoresis unit; Bio-Rad Laboratories) based on the method of Laemmli (31,32). Twelve to fourteen percent gels under reducing conditions were used to resolve the heavy and light chains of the PICs and to assess qualitatively the extent of intra-antibody cross-linking or aggregation (or both). In addition, 5% gels under nonreducing conditions were used to resolve the various levels of PEGylation of the PICs, to assess qualitatively the extent of interantibody aggregation, and to quantify the residual amounts of free photosensitizer impurity in the final PIC preparations. Gels were imaged and analyzed using a CCD camera gel-viewing system (ChemImager, Alpha Innotech Corporation, San Leandro, CA). PICs and free BPD were seen as green bands with white light illumination and as red fluorescent bands with UV light excitation. The UV light source was filtered with 2 cm of 250 g/L $\text{CuSO}_4 \cdot 5\text{H}_2\text{O}$ to remove the background infrared radiation of the lamps, and the red fluorescent bands on the gel were detected using a long-wavelength-pass filter (>620 nm). After fluorescence imaging, gels were Coomassie stained and imaged using white light illumination to visualize antibody protein content and protein marker bands.

Photophysical characterization of the PICs. Fluorescence quantum yields. Relative fluorescence quantum yields for free BPD and for various PIC samples with varying BPD–antibody (BPD:Ab) molar loading ratios were calculated from the ratios of the slopes of fluorescence emission intensity versus absorbance plots. The fluorescence emission intensity versus absorbance plot for a given sample was generated by measuring the emission intensities of a series of dilute solutions prepared from a concentrated stock solution of the sample. Typically four to five different dilutions of a given sample were prepared in 50% DMSO–50% aqueous solutions with absorbances ranging from 0 to ~ 0.1 cm^{-1} at the excitation wavelength 428 nm, which is centered near the absorbance peak maximum of the Soret band of BPD. Fluorescence emission intensity was measured as the area under the fluorescence emission peak in the 650–800 nm range. Steady state fluorescence spectra were acquired using a Spex FluoroMax spectrofluorometer (Spex Industries, Inc., Edison, NJ).

Fluorescence lifetime measurement. Fluorescence decay signals of free BPD and of various PIC preparations with varying BPD–Ab molar loading ratios were measured using a TimeMaster fluorescence lifetime spectrometer, operated in its StrobeMaster stroboscopic mode (Photon Technology International, Inc., Monmouth Junction, NJ). The StrobeMaster stroboscopic system is based on a technique described by Bennett (33). The excitation source was a N_2 (30%)–He nanosecond lamp. Samples were prepared in 50% DMSO–50% aqueous solutions and were adjusted by dilution to an absorbance of approximately 0.4 cm^{-1} at ~ 690 nm to ensure that all solutions contained roughly equal amounts of BPD content. Before recording fluorescence decay signals, a BaSO_4 scattering solution was used to measure the nanosecond lamp temporal profile, *i.e.* the instrument response function (IRF). The experimental fluorescence decays were then acquired with the emission monochromator set at 700 nm. Because sample solutions were excited with the full N_2 (30%)–He lamp spectrum (~ 300 – 400 nm), a long-pass filter (>579 nm) was placed in front of the emission monochromator to eliminate second-order grating effects. The IRF was then used to fit the experimental fluorescence decay signals by an iterative reconvolution procedure, assuming either a monoexponential or a biexponential free-fluorescence decay. The fitting procedure was based on the Marquardt algorithm (34,35).

Cellular uptake. Cells were plated in 2 mL of media in 35 mm tissue culture dishes at densities such that the cells reached $\sim 90\%$ confluence at the end of a 3 day growth period. After an initial period of at least 14–20 h, which allowed for cells to attach and begin dividing, incubation with PIC or free BPD was initiated by replacing the original 2 mL of media with 2–4 mL of media containing PIC or free BPD. From this point onward, cells were handled under low-light conditions to avoid photosensitizing the cells or photobleaching the photosensitizer. Incubations were done at 37°C and were begun with respect to the end of the 3 day growth period.

At the end of the 3 day growth period, the media containing PIC or free BPD was removed, and cells were washed twice with 2 mL of PBS. Cell samples were then collected and analyzed. Cells were lifted off culture dishes using either trypsin or a scraper, and 1 mL cell suspensions in culture medium (without any fetal bovine serum) were prepared from each dish. A 0.4 mL aliquot of each 1 mL cell suspension was solubilized in 2 mL of 1 M NaOH–1% SDS in a disposable fluorometer cuvette. To quantitate the BPD content of the solubilized cell samples, the fluorescence emission intensities

of the samples were compared with those of free-BPD standards. Fluorescence measurements were performed as previously described. The remaining 0.6 mL of each cell suspension was used to do a cell count using a hemacytometer and to assay for cell protein content by a Bradford-type protein assay. Alternatively, cells were removed from culture dishes by incubating the cells with 100 μL of lysis buffer (5 mM disodium ethylenediaminetetraacetic acid, 10 mM Tris base, 150 mM NaCl, 1% Triton X-100, 0.1% protease inhibitor cocktail solution [Sigma-Aldrich] and 1 mM phenylmethanesulfonyl fluoride; protease inhibitors were added just before use) per dish at 37°C for 5–10 min, followed by the addition of 900 μL of deionized–distilled H_2O per dish. Any remaining adherent cellular debris was scraped off and pipetted a few times to ensure thorough removal of cellular material. This yielded a 1 mL solubilized cell sample from each dish. Half a milliliter of each solubilized cell sample was mixed with 2 mL of 1 M NaOH–1% SDS in a disposable fluorometer cuvette to measure BPD content *via* fluorescence quantitation. The remaining 0.5 mL of each solubilized cell sample was used to do a protein assay. To relate protein content to the number of cells, sets of control cell dishes that had not been treated with PIC or free BPD were prepared solely to estimate the conversion parameter, number of cells per milligram of cell protein. The value of this parameter, which varied for the different cell lines, was measured in the following manner. First, 1 mL cell suspensions in culture medium, prepared from one set of control cell dishes, were counted using a hemacytometer. Second, 1 mL solubilized cell samples in lysis buffer, prepared from a corresponding set of control cell dishes, were assayed for protein content.

Phototoxicity. Cells were plated in 2 mL of media in 35 mm tissue culture dishes at densities such that the cells reached approximately 60–80% confluence at the end of a 3 day growth period. After an initial period of at least 14–20 h, which allowed for cells to attach and begin dividing, incubation with PIC or free BPD was initiated by replacing the original 2 mL of media with 2–4 mL of media containing PIC or free BPD. Incubations were done at 37°C and were begun with respect to the end of the 3 day growth period. At the end of the 3 day growth period, the media containing PIC or free BPD were removed. Cells were washed once with 2 mL of DPBS, and 2 mL of fresh media were added back to each dish. Cells were then immediately irradiated with the requisite light dose. After irradiation, cells were incubated overnight at 37°C and then assayed for viability by colorimetric MTT (3-(4,5-dimethylthiazol-2-yl)-2,5-diphenyltetrazolium bromide) assay (36). Except for the intended light dose, care was taken to protect the cells from light exposure at all times.

The radiation source was a dye laser pumped by an argon ion laser (models CR-599 and Innova 100, respectively, Coherent Inc., Palo Alto, CA). The laser dye was DCM [4-(dicyanomethylene)-2-methyl-6-(*p*-dimethylaminostyryl)-4H-pyran], and the dye laser emission was tuned to 690 nm. Alternatively, a 687 nm laser diode (model SDL 7432, SDL Inc., San Jose, CA) was used as the radiation source. To achieve homogeneous irradiation of the cells, 690 nm light from the laser was focused through a $10\times$ microscope lens onto the end of an optical fiber that delivered light through an inverted $4\times$ microscope lens to give a 35 mm diameter illumination spot. The illumination spot was projected up through the bottom of the culture dishes. Fluence rates ranged from approximately 20–40 mW/cm^2 .

Competition studies. In tissue culture experiments with EGFR-over-expressing A-431 cells, binding of the C225 PIC to the EGFR was competed with varying amounts of the unmodified C225 antibody. Competition experiments were conducted using saturating amounts of C225 PIC coincubated with equal or greater amounts of unmodified antibody. Typically, the unmodified antibody concentration was varied from one to four times the concentration of the C225 PIC.

RESULTS AND DISCUSSION

Preparation and purity characterization of the PICs

Although many previous PIC studies have used predominantly aqueous solutions to prepare conjugates (8), initial efforts in this investigation to prepare PICs using predominantly aqueous buffered solutions failed because of the hydrophobic and aggregative properties of BPD. In fact, even when the active ester of BPD was prepared as a sulfo-NHS derivative, which enhanced its water solubility, conjugation reaction yields remained low in predominantly aqueous solutions, and the resulting PICs could not be

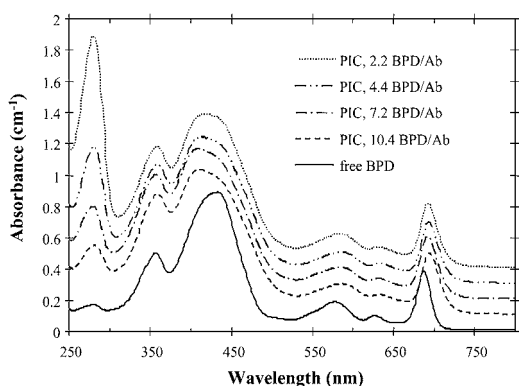


Figure 1. Ground state absorption spectra of free BPD and of C225 PICs of varying BPD–Ab molar ratios. Samples were prepared in 50% DMSO–50% aqueous solutions. The BPD content of the free-BPD sample corresponds to approximately 9.5 $\mu\text{g}/\text{mL}$. To permit clearer observation of all spectra, each spectrum has been offset successively by 0.1 cm^{-1} absorbance units.

adequately purified. Furthermore, in terms of delivering therapeutic payloads of the photosensitizer, these low-purity conjugates exhibited poor specificity for the designated target cell lines (results not shown).

This poor specificity was attributed to the low purity of the initial conjugate preparations. Obtaining adequately purified PIC necessitated overcoming the photosensitizer's tendencies to self-aggregate and bind noncovalently to the hydrophobic pockets of proteins (6,37). Preliminary solubility studies revealed that free-BPD changes from a predominantly aggregated state to a predominantly disaggregated monomeric state as solution composition is increased above approximately 40% DMSO (data not shown). Similar observations have been reported previously for BPD in aqueous methanol solutions (37). In addition, antibody stability studies in DMSO–aqueous buffered solutions demonstrated that antibody remains soluble and stable for DMSO content up to 50% but aggregates and denatures irreversibly for DMSO content above approximately 60% (data not shown). On the basis of these observations, it was determined that a 50% DMSO–50% aqueous two-solvent system would be an ideal solution for synthesis and purification of BPD-labeled PIC. Moreover, polar aprotic solvents such as DMSO are known to increase the kinetics and efficiency of a number of organic reactions (38).

PICs with BPD–Ab molar loading ratios ranging from approximately 2 up to 11 were prepared in this study. The purity of the PIC preparations, assessed by SDS-PAGE gel fluorescence imaging analysis, was approximately less than 5% residual free photosensitizer impurity. In fact, this measurement of purity represents an upper-bound estimate because no efforts were made to account for fluorescence quenching of the conjugated photosensitizer in the gels when estimating PIC purity. Typical absorbance spectra of a series of C225 PICs with varying BPD–Ab molar loading ratios are shown in Fig. 1. The spectra show that the protein absorption peak at 280 nm gradually decreases in the expected manner relative to the photosensitizer absorption peaks as the PIC-loading ratio increases. The yield of the photosensitizer conjugation reaction was approximately 75% for the preparation of PICs with BPD–Ab molar loading ratios of 2. However, the photosensitizer conjugation reaction yield dropped below 45% for the preparation of PICs with BPD–Ab molar loading ratios greater than 10. Moreover, when attempts were made to increase BPD–Ab

molar loading ratios beyond approximately 11, the residual free photosensitizer impurity of the PIC preparations increased above 10%, even after extensive efforts to purify the conjugates. These observations were an indication that antibody lysine amino groups became less available as higher BPD–Ab molar loading ratios were attempted. Because the focus of this study was to investigate the activity of the PICs themselves rather than the activity of the noncovalently associated photosensitizer impurity present in the PIC preparations, only PIC preparations with residual photosensitizer impurity of less than about 5% were used in cell studies.

Role of PEGylation of the PICs

It was not necessary to PEGylate the PICs to maintain their solubility in 50% DMSO–50% aqueous solutions for a short-term storage period of a few days. However, unPEGylated PICs gradually formed large insoluble aggregates during long-term storage in 50% DMSO solutions. In addition, it was not possible to transfer a concentrated solution of unPEGylated PIC from 50% DMSO to purely aqueous solutions without forming large insoluble aggregates. To overcome these problems the antibody was PEGylated with a special two-branched PEG-NHS ester before labeling with BPD-NHS ester. Figures 2 and 3 show how the PEGylation reaction yields a mixture of species in a typical C225 PIC preparation. PEGylation essentially resulted in splitting of the single major protein band of the original unmodified antibody into a ladder of three major PIC protein bands of roughly equal or higher molecular weight. From the gel shown in Fig. 2, the unmodified antibody molecular weight was estimated to be 170 kDa, and the apparent molecular weights of the major PIC protein bands were estimated to be 179, 198 and 218 kDa. The spacing of the PIC protein bands is roughly 20 kDa, whereas the molecular weight of the two-branched PEG is known to be 10 kDa. This indicates that the migration characteristic of PEGylated antibody on SDS-PAGE gels is somewhat different from that of unPEGylated globular protein standards. We conclude that the major PIC protein bands correspond to 0, 1 and 2 PEG moieties per PIC molecule. It is noteworthy that a significant fraction of the species present in the PIC preparations consisted of unPEGylated PIC, and yet the PIC preparations as a whole remained soluble in purely aqueous solutions. This suggests that there may exist a maximum limit for the proportion of unPEGylated material that can be present in a PIC preparation beyond which aggregation and precipitation problems are manifested. In Fig. 3 it can also be clearly seen that more highly PEGylated PICs and possibly other heavy-molecular weight aggregates were present in the PIC preparations as minor species. However, no efforts were made to remove these minor species before using the PICs in cell experiments.

PIC integrity and the importance of NHS ester purification

It was of interest to investigate the structural integrity of the antibody at all stages of the conjugation procedure given that the overall process of producing the PICs involved several reaction and purification steps. Figure 3 shows how various treatments of the antibody affected its migration characteristics on a nonreducing SDS-PAGE gel. Lane 2 shows that treatment of C225 with 50% DMSO did not affect the antibody's structural integrity in any way. As already discussed above, lane 3 shows that PEGylation of the antibody resulted in splitting of the single major protein band of the original

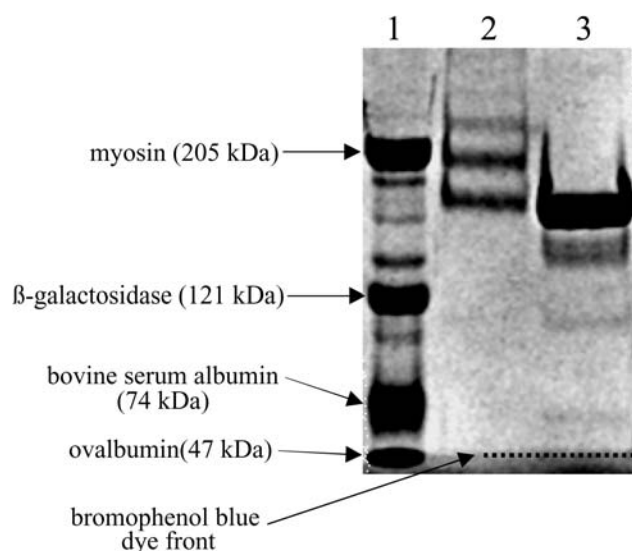


Figure 2. Five percent nonreducing SDS-PAGE gel for estimating molecular weights of the various major species in a C225 PIC preparation. Lanes: (1) protein standards; (2) C225 PIC, 7 BPD/antibody; and (3) unmodified C225.

unmodified antibody into a ladder of three major protein bands, which appear to correspond to 0, 1 and 2 PEG moieties per antibody.

Previous photosensitizer conjugate studies (1,4,21–26,39–42) used unpurified active ester preparations or active ester preparations of unspecified purity in the conjugation reactions. Consequently, in lanes 4–7 of Fig. 3, the effects of treating antibody either with a mixture of EDC and NHS or with unpurified crude BPD-NHS active ester were examined and compared with PIC prepared from purified BPD-NHS active ester. Treatment of the antibody with unpurified crude BPD-NHS active ester was performed in the same manner as treatment of the antibody with purified BPD-NHS active ester, except that no efforts were made to purify the crude active ester product. Treatment of the antibody with EDC and NHS was performed in the same manner as treatment of the antibody with unpurified crude BPD-NHS active ester, except that no BPD was added to the mixture of EDC and NHS. Lane 4 shows that reaction of the antibody with EDC and NHS yielded a fraction of intermolecularly cross-linked antibody aggregates. Moreover, the nonintermolecularly cross-linked fraction of the antibody that was treated with the EDC–NHS mixture appeared to migrate slightly faster than the untreated antibody in lane 1, and the protein bands were somewhat streaked. These effects appear to be indications of intramolecular antibody cross-links, which can be expected given that antibodies contain large numbers of lysines in close proximity to glutamic and aspartic acid residues. Lane 5 shows that PEGylation of the antibody before treatment with the EDC–NHS mixture greatly suppressed intermolecular cross-links, but the fact that the major protein bands were slightly downshifted and streaked in comparison with lane 3 suggests that PEGylation did not prevent intramolecular cross-links. Lane 7 shows that PIC prepared from unpurified BPD-NHS exhibited a similar migration pattern to PEGylated antibody treated with the EDC–NHS mixture. In addition, a significant amount of free BPD at the bottom of lane 7 in Fig. 3B shows that PIC prepared from unpurified BPD-NHS could not be thoroughly purified even after gel filtration in 50% DMSO. In contrast, lane 6

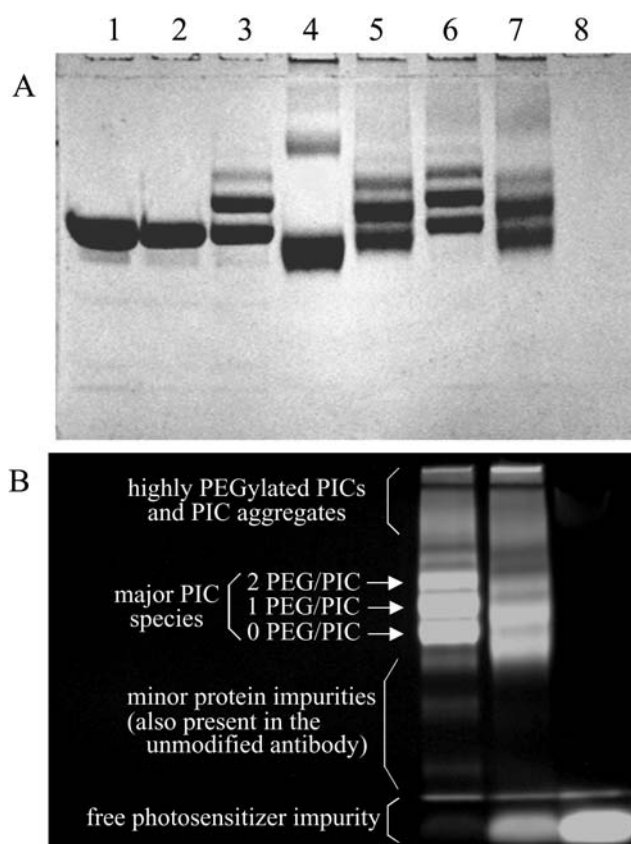


Figure 3. Five percent nonreducing SDS-PAGE gel of various conjugate preparations and control samples. A: White light illumination image of Coomassie stained gel. B: Fluorescence image of the same gel before Coomassie staining. Lanes: (1) unmodified C225; (2) 50% DMSO-treated C225; (3) PEGylated C225; (4) EDC + NHS-treated C225; (5) PEGylated and EDC + NHS-treated C225; (6) C225 PIC made with purified BPD-NHS, 7 BPD/antibody; (7) C225 PIC made with unpurified BPD-NHS; and (8) free BPD.

shows that PIC prepared from purified BPD-NHS contained significantly less free photosensitizer impurity, and the protein bands were not streaked or downshifted. Taken together, the aforementioned observations suggest that thorough purification of the BPD-NHS active ester was crucial in terms of preventing undesirable cross-linking reactions and obtaining high-purity PIC preparations containing less than about 5% noncovalently associated photosensitizer impurity, especially when high BPD–Ab molar loading ratios were desired.

The various treatments of the antibody were also analyzed on 12–14% reducing SDS-PAGE gels (data not shown). Under reducing conditions the heavy and light chains of the antibody could be resolved. Treatment of the antibody with DMSO did not affect the resolution of the heavy and light chains of the antibody in any way. However, unlike the analysis of PEGylated antibody on nonreducing gels, analysis of PEGylated antibody on reducing gels was not as clear-cut to interpret. PEGylated antibody on reducing gels resolved into the two major bands that corresponded with the heavy and light chains of the antibody, but the only evidence that the antibody had been PEGylated was the appearance of two faint bands slightly above the heavy chain. Antibody that had been treated with the mixture of EDC and NHS aggregated at the interface of the stacking and resolving gels for the most part, and

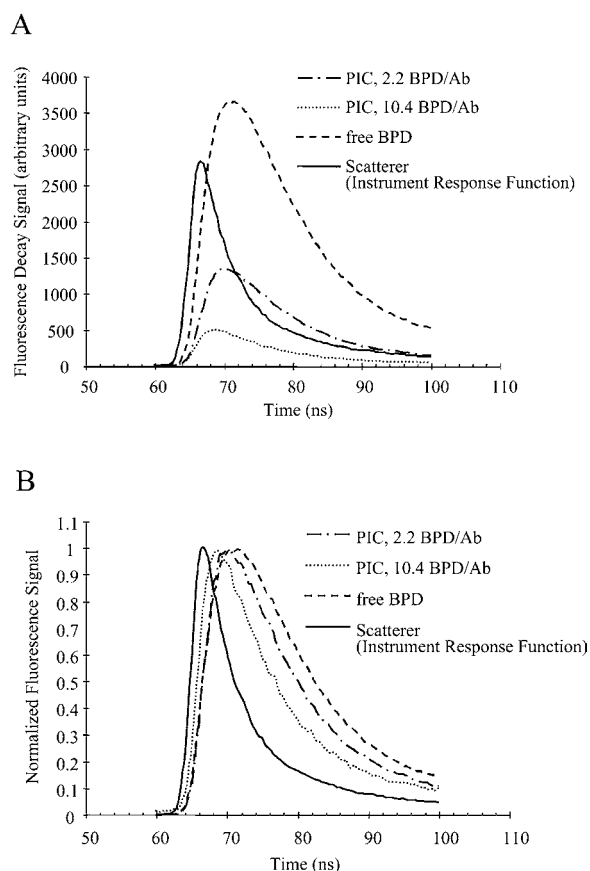


Figure 4. Fluorescence decays of two different C225 PICs and of free BPD in 50% DMSO–50% aqueous solutions. The sample solutions were the same as those corresponding to the absorption spectra shown in Fig. 1. A: Unnormalized fluorescence decay signals. B: Normalized fluorescence decay signals.

only a small fraction of the sample resolved as heavy and light chains. By comparison, PIC prepared from purified BPD-NHS active ester migrated in a very similar manner to PEGylated antibody, and only a small fraction aggregated at the interface of the stacking and resolving gels. These observations further support the notion that thorough purification of the BPD-NHS active ester was crucial in terms of preventing undesirable intramolecular and intermolecular cross-linking of the antibody.

Photophysical characterization of the PICs

Some previous PIC studies have claimed that conjugation does not significantly affect the photosensitizer's photophysical and photochemical properties, whereas others have shown that the photosensitizer's capacity to generate phototoxic species is quenched subsequent to conjugation (8). Lack of consensus among various PIC investigations regarding the effects that conjugation has on a photosensitizer's photophysical and photochemical properties may be due in part to the different choices of photosensitizers and PIC designs, the different photophysical and photochemical methods used to characterize the PICs, and the presence of significant amounts of noncovalently associated photosensitizer impurities in the PIC preparations. In this study, relative fluorescence quantum yields and fluorescence decay signals for free BPD and for various high-purity BPD PIC preparations were measured to assess how conjugation to the antibody affected the

ability of BPD to generate phototoxic species. Although fluorescence is a photophysical property of the singlet excited state of a photosensitizer, fluorescence quantum yields and decay times generally correlate with a photosensitizer's ability to intersystem cross and generate phototoxic species *via* energy transfer from its lowest-lying excited triplet state. The reason for this correlation is that a photosensitizer's phototoxic quantum yield is usually directly proportional to its triplet quantum yield, and both the triplet and fluorescence quantum yields are directly proportional to the photosensitizer's singlet excited state lifetime (8).

Fluorescence properties were measured in 50% DMSO–50% aqueous solutions to overcome the tendency of BPD to aggregate in purely aqueous solution. This allowed an investigation of the quenching effects that occur as a result of covalent anchorage of BPD onto the antibody as opposed to the quenching effects that occur as a result of the photosensitizer's noncovalent aggregative interactions. Previous PIC investigations examined the photophysical and photochemical properties of PICs in predominantly aqueous solutions and did not distinguish between these two types of quenching effects (8). However, it is important to distinguish between these two effects given that in an *in vivo* setting, noncovalent interactions of the photosensitizer are most likely disrupted by interactions with serum proteins and the lipid bilayers of cells, whereas covalent linkage of the photosensitizer onto the antibody cannot be disrupted except by hydrolytic or enzymatic processes.

Unnormalized and normalized fluorescence decays that are representative of the various PICs and of free BPD are shown in Fig. 4A and B, respectively. Figure 4A shows that the intensities of the PIC fluorescence decay signals were significantly reduced compared with that of free BPD and that the intensities of the PIC fluorescence decay signals decreased as the BPD–Ab molar loading ratio was increased. Figure 4B shows that the PIC fluorescence decay signals were significantly shorter lived than that of free BPD and that the PIC fluorescence decay lifetimes decreased as the BPD–Ab molar loading ratio was increased. The free-BPD fluorescence decay signal was best fit by a mono-exponential, and the PIC fluorescence decay signals were best fit by biexponentials. The weighted-average fluorescence decay lifetimes for free BPD and for PICs with BPD–Ab molar loading ratios of 2.2, 4.4, 7.2 and 10.4 were 6.02, 2.98, 2.10, 1.42 and 1.38 ns, respectively. Relative fluorescence quantum yields correlated well with fluorescence decay lifetimes. Relative fluorescence quantum yields for free BPD and for PICs with BPD–Ab molar loading ratios of 2.2, 4.4, 7.2 and 10.4 were 1.00, 0.314, 0.204, 0.152 and 0.111, respectively.

These spectroscopic observations show that covalent conjugation of BPD to antibodies effectively results in static concentration quenching (43). This is not surprising given that photosensitizer molecules must necessarily pack closer to each other on the antibody as the BPD–Ab molar loading ratio of the PIC is increased. Incidentally, it is also possible to discern quenching-related effects in the absorption spectra shown in Fig. 1. Whereas the absorption spectrum for free BPD resembles that of monomeric BPD, the dye portion of the absorption spectra for the PICs resembles that of aggregated BPD (37). These data confirm that there is a major trade-off in terms of delivering as much photosensitizer as possible per PIC carrier and at the same time avoiding quenching effects. For the PICs developed in this investigation, the data clearly show that it was not possible to achieve relatively high BPD–Ab molar loading ratios without

appreciably quenching the photophysics and, presumably, the photochemistry of the PICs.

Cellular uptake

Cellular uptake studies are shown in Fig. 5. For these preliminary uptake studies, the conjugation procedure had not yet been fully optimized. Therefore, although it was found in subsequent experiments that a PEG-NHS-antibody molar ratio of approximately 2 in the conjugation was sufficient to maintain PIC solubility in aqueous solutions, in these preliminary cellular uptake studies the PICs were either unPEGylated or prepared using PEG-NHS-antibody molar ratios of approximately 4. In addition, although the unPEGylated PICs were stable in 50% DMSO solutions for a period of a few days, completely aqueous concentrated solutions of the unPEGylated PICs could not be prepared without forming large insoluble aggregates. Consequently, to use the unPEGylated PICs in preliminary tissue culture studies, it was necessary to expose cells to ~0.7% DMSO during incubations. Moreover, the PICs used in these early studies were still prepared using unpurified crude BPD-NHS, which necessitated that the molar loading ratio of the PICs be limited to roughly 4 BPD/antibody to ensure acceptable purity of the PICs ($\leq 5\%$ non-covalently associated photosensitizer impurity).

Despite the fact that the experimental conditions for the preliminary cellular uptake studies were not fully optimized, these initial studies yielded several important insights. First, PEGylation reduced nonspecific J774 macrophage uptake of the PICs by a factor of approximately 2–3. This effect was most likely a result of the dramatically reduced aggregation of the PEGylated PIC preparations. Second, the anti-EGFR C225 PICs were taken up by the EGFR-overexpressing A-431 cells but not by the EGFR-negative NR6 cells. Likewise, nonspecific RbIgG PICs were not taken up by either the A-431 cells or the NR6 cells to any significant extent. These results demonstrate that except for some nonspecific macrophage uptake, which was appreciably reduced by PEGylating the PICs, the C225 PICs were capable of specifically targeting EGFR-overexpressing cells in the intended manner. In contrast, free BPD exhibited no apparent specificity for any of the various cell lines.

Phototoxicity

Preliminary phototoxicity studies were conducted using EGFR-overexpressing A-431 cells and EGFR-negative NR6 cells. For these phototoxicity studies the conjugation procedure had been optimized. A PEG-NHS-antibody molar ratio of approximately 2 was used to prepare the PICs, which allowed the PICs to be transferred to purely aqueous buffer without forming insoluble aggregates. Therefore, unlike the preliminary cellular uptake studies, it was unnecessary to expose cells to even small amounts of DMSO during incubations. Furthermore, the PICs were prepared using purified BPD-NHS, which permitted higher BPD–Ab molar loading ratios without sacrificing PIC purity. Consequently, PICs with molar loading ratios of ~7 BPD/antibody were used in these phototoxicity studies. Although preliminary cellular uptake measurements revealed that total BPD uptake for A-431 cells using the C225 PIC was comparable with that achieved using the free photosensitizer after a 14 h incubation period (Fig. 5), initial phototoxicity experiments showed that high levels of cell killing could not be achieved with the C225 PIC unless the incubation period was prolonged significantly beyond 14 h. In contrast,

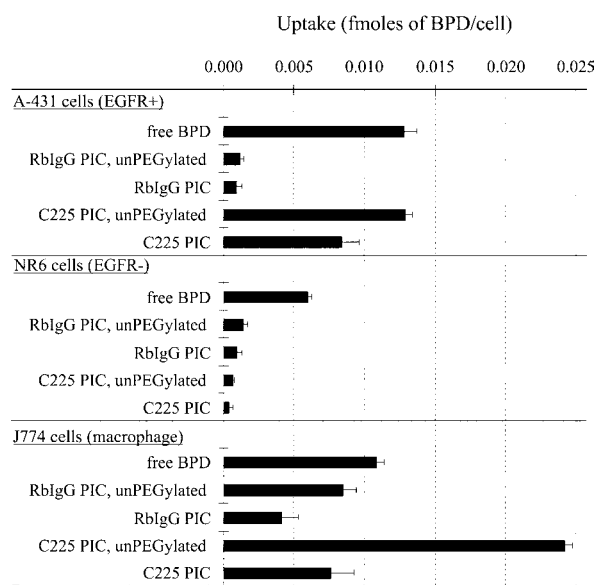


Figure 5. Cellular uptake studies. Cellular uptake measurements for three different cell lines were conducted using four different types of PIC as well as free BPD. Cells were incubated with 140 nM BPD content of the PIC or free BPD for 14 h at 37°C in the presence of 0.7% DMSO (see text). Uptakes can be converted to femtomoles of BPD per milligram of cell protein using the following conversion factors: 1.7×10^6 cells/mg cell protein for A-431s, 1.5×10^6 cells/mg cell protein for NR6s and 3.0×10^6 cells/mg cell protein for J774s.

phototoxic cell killing with the free photosensitizer was greater than 90% even for incubation periods much shorter than 6 h (data not shown). These observations were not surprising in view of the photophysical findings. Presumably, at longer incubation times, the PIC is degraded to produce significant amounts of dequenched photosensitizer. Therefore, a 40 h incubation period with the C225 PIC was used for the cell killing studies reported here.

Figure 6A shows that it was possible to achieve a 90% reduction in A-431 cell viability with the C225 PIC by using a light dose of 20 J/cm² and that the phototoxic effects of the PIC were effectively competed by coinubation with unmodified C225 antibody. The fact that competition with unmodified C225 antibody reduced the phototoxic effects of the C225 PIC demonstrates that this PIC's activity is predominantly mediated by its specific binding to the EGFR. It is noteworthy that cells treated with unmodified C225 antibody alone exhibited a slight reduction in viability. Similarly, cells treated with the C225 PIC and coinubated with unmodified C225 antibody but not exposed to light also exhibited a slight reduction in viability. These observations appear to be in agreement with previous results that show that the unmodified C225 antibody by itself possesses growth inhibitory effects (44). In addition, it is important to note that phototoxic killing either with free BPD or with free BPD mixed with unmodified C225 resulted in greater than 99% reduction in A-431 cell viability, which was significantly greater than the killing achieved with the C225 PIC. However, these observations are not entirely surprising given that conjugation of BPD to C225 antibody no doubt radically modifies the cellular uptake kinetics, subcellular localization characteristics, and photophysical properties of BPD (*e.g.* as previously discussed, the intact conjugates exhibit appreciable static concentration quenching). Finally, Fig. 6B shows that under similar conditions,

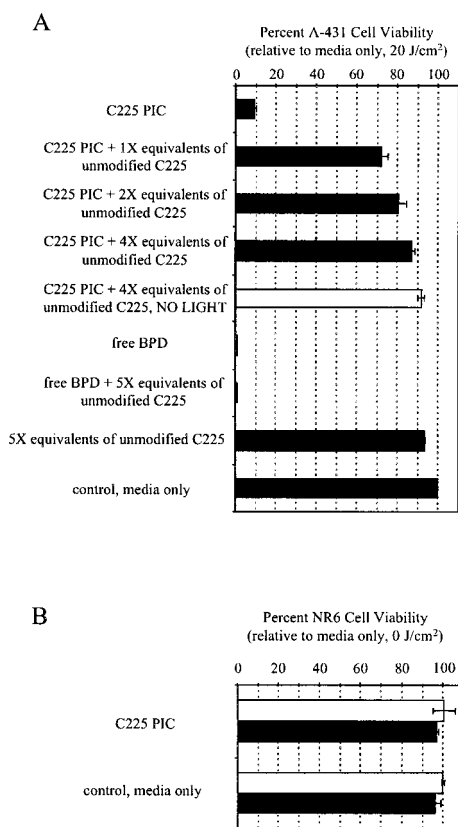


Figure 6. Phototoxicity experiments. The molar loading ratio of the PIC was ~ 7 BPD/antibody. Light doses were either 0 J/cm^2 (\square) or 20 J/cm^2 (\blacksquare). A: EGFR-overexpressing A-431 cells were incubated at 37°C for 40 h with C225 PIC (approximately 20 nM antibody content or, equivalently, 140 nM BPD content), either in the absence or in the presence of $1\times$, $2\times$ or $4\times$ equivalents of unmodified C225 antibody (approximately 20 , 40 and 80 nM antibody content, respectively). Control experiments included 140 nM free BPD, 140 nM free BPD + $5\times$ equivalents (100 nM antibody content) of unmodified C225, $5\times$ equivalents of unmodified C225 and media only. B: EGFR-negative NR6 cells were incubated at 37°C for 40 h with C225 PIC (approximately 40 nM antibody content or, equivalently, 280 nM BPD content).

the C225 PIC had no noticeable phototoxic effect on EGFR-negative NR6 cells.

CONCLUSIONS

To summarize, several major problems with the design, synthesis and purification of PICs have been dealt with in this investigation. For the most part, the problems that had to be overcome stemmed from the incompatible solubilities of photosensitizer and antibody. Whereas the best photosensitizers for PDT are usually hydrophobic and lipophilic, antibodies and immunoconjugates must remain water soluble and disaggregated to reach their designated targets in an efficient manner *via* the circulation. Because many of the previous studies of PICs did not devise conjugation methods that were capable of circumventing the incompatible solubilities of photosensitizer and antibody, the conjugate preparations in these earlier studies very likely contained significant amounts of aggregated material and noncovalently associated photosensitizer impurities. Consequently, interpretation of the observed biological effects of PICs in previous PIT studies has been difficult, especially for *in vitro* studies, because the effects of the actual conjugates

cannot be clearly distinguished from the effects of noncovalently associated photosensitizer impurities or large aggregates (or both) that may have been present in the PIC preparations. In turn, it has been difficult to discern from these previous PIT studies what measures must be taken to improve the overall performance of PIC constructs.

This study describes a method for producing reasonably purified PICs. However, it is not a simple matter to establish what attributes a PIC should possess to achieve the best biological response. It is possible that thorough removal of noncovalently associated photosensitizer impurities may not be necessary to produce PIC preparations of clinical utility (even the most widely used photosensitizer in clinical PDT, Photofrin[®], consists of a heterogeneous porphyrin mixture [45,46]). However, the presence of such impurities has made it difficult to study the true nature of the conjugates themselves. Now the availability of purified PICs should allow us to study some of these variables more rigorously and should make more in-depth studies of the biological behavior of the PICs much easier to interpret. On the basis of our experience with lower-purity PIC preparations, it appears that the real value of these purified conjugates may be in providing significantly enhanced selectivity, which is critical for treatment of complex anatomical sites such as the peritoneal cavity. Future studies of these PEGylated BPD-C225 PICs will involve *in vivo* testing as well as additional *in vitro* experiments to examine in greater detail various issues concerning PIC dosimetry and mechanisms of action.

Acknowledgements—We thank Drs. Robert Gilmont, Riley Rees and Stephen Rand, who helped to initiate this work, Drs. Krishnan Rajagopalan and Richard Lawton, who provided guidance regarding synthesis and purification issues, Dr. Robert Redmond, who provided valuable discussion and advice regarding photophysical and photochemical measurements, and Dr. Michael Hamblin for his stimulating and challenging discussions concerning photosensitizer conjugates. We also thank ImClone Systems Incorporated for their generous gift of C225 anti-EGFR antibody and QLT PhotoTherapeutics Incorporated for their generous gift of BPD. M.S. gratefully acknowledges the support he received throughout his Ph.D. studies from the Whitaker Foundation's Biomedical Engineering Graduate Fellowship program. A National Institutes of Health grant R01AR40352 also supported this work.

REFERENCES

- Hamblin, M. R., J. L. Miller and T. Hasan (1996) Effects of charge on the interaction of site-specific photoimmunoconjugates with human ovarian cancer cells. *Cancer Res.* **56**, 5205–5210.
- DeLaney, T. F., W. F. Sindelar, Z. Tochner, P. D. Smith, W. S. Friauf, G. Thomas, L. Dachowski, J. W. Cole, S. M. Steinberg and E. Glatstein (1993) Phase I study of debulking surgery and photodynamic therapy for disseminated intraperitoneal tumors. *Int. J. Radiat. Oncol. Biol. Phys.* **25**, 445–457.
- Duska, L. R., M. R. Hamblin, J. L. Miller and T. Hasan (1999) Combination photoimmunotherapy and cisplatin: effects on human ovarian cancer *ex vivo*. *JNCI* **91**, 1557–1563.
- Mew, D., C. K. Wat, G. H. N. Towers and J. G. Levy (1983) Photoimmunotherapy: treatment of animal tumors with tumor-specific monoclonal antibody-hematoporphyrin conjugates. *J. Immunol.* **130**, 1473–1477.
- Hasan, T. (1992) Photosensitizer delivery mediated by macromolecular carrier systems. In *Photodynamic Therapy: Basic Principles and Clinical Applications* (Edited by B. W. Henderson and T. J. Dougherty), pp. 187–200. Marcel Dekker, Inc., New York.
- Sternberg, E. D., D. Dolphin and C. Brückner (1998) Porphyrin-based photosensitizers for use in photodynamic therapy. *Tetrahedron* **54**, 4151–4202.
- Yarmush, M. L., W. P. Thorpe, L. Strong, S. L. Rakestraw, M. Toner

- and R. G. Tompkins (1993) Antibody targeted photolysis. *Crit. Rev. Ther. Drug Carrier Syst.* **10**, 197–252.
8. Savellano, M. D. (2000) Photodynamic Targeting with Photosensitizer Immunocjugates. Ph.D. Thesis, University of Michigan, Ann Arbor, MI. [Available online from UMI Dissertations Publishing]
 9. Richter, A. M., B. Kelly, J. Chow, D. J. Liu, G. H. N. Towers, D. Dolphin and J. G. Levy (1987) Preliminary studies on a more effective phototoxic agent than hematoporphyrin. *JNCI* **79**, 1327–1331.
 10. Aveline, B., T. Hasan and R. W. Redmond (1994) Photophysical and photosensitizing properties of benzoporphyrin derivative monoacid ring A (BPD-MA). *Photochem. Photobiol.* **59**, 328–335.
 11. Schmidt-Erfurth, U. and T. Hasan (2000) Mechanisms of action of photodynamic therapy with verteporfin for the treatment of age-related macular degeneration. *Surv. Ophthalmol.* **45**, 195–214.
 12. Fan, Z. and J. Mendelsohn (1998) Therapeutic application of anti-growth factor receptor antibodies. *Curr. Opin. Oncol.* **10**, 67–73.
 13. Harari, P. M. and S. M. Huang (2000) Modulation of molecular targets to enhance radiation. *Clin. Cancer Res.* **6**, 323–325.
 14. Mendelsohn, J. and Z. Fan (1997) Epidermal growth factor receptor family and chemosensitization. *JNCI* **89**, 341–343.
 15. Huang, S. M., J. M. Bock and P. M. Harari (1999) Epidermal growth factor receptor blockade with C225 modulates proliferation, apoptosis, and radiosensitivity in squamous cell carcinomas of the head and neck. *Cancer Res.* **59**, 1935–1940.
 16. Harari, P. M. and S. M. Huang (2001) Head and neck cancer as a clinical model for molecular targeting of therapy: combining EGFR blockade with radiation. *Int. J. Radiat. Oncol. Biol. Phys.* **49**, 427–433.
 17. Mendelsohn, J. (2000) Jeremiah Metzger lecture: targeted cancer therapy. *Trans. Am. Clin. Climatol. Assoc.* **111**, 95–111.
 18. de Bono, J. S. and E. K. Rowinsky (2002) The ErbB receptor family: a therapeutic target for cancer. *Trends Mol. Med.* **8S**, S19–S26.
 19. Perkins, A. S. and D. F. Stern (1997). In *Cancer: Principles and Practice of Oncology*, V (Edited by T. DeVita, S. Hellman and S. A. Rosenberg), pp. 79–102. Lippincott-Raven, Philadelphia, PA.
 20. Garber, K. (2000) New discoveries still abundant in monoclonal antibody research. *JNCI* **92**, 1462–1464.
 21. Levy, J. G., D. Dolphin and J. K. Chow (1989) Wavelength-specific cytotoxic agents. U.S. patent 4,883,790.
 22. Jiang, F. N., S. Jiang, D. Liu, A. Richter and J. G. Levy (1990) Development of technology for linking photosensitizers to a model monoclonal antibody. *J. Immunol. Methods* **134**, 139–149.
 23. Jiang, F. N., D. J. Liu, H. Neyndorff, M. Chester, S. Jiang and J. G. Levy (1991) Photodynamic killing of human squamous cell carcinoma cells using a monoclonal antibody-photosensitizer conjugate. *JNCI* **83**, 1218–1225.
 24. Jiang, F. N., B. Allison, D. Liu and J. G. Levy (1992) Enhanced photodynamic killing of target cells by either monoclonal antibody or low density lipoprotein mediated delivery systems. *J. Control. Release* **19**, 41–58.
 25. Jiang, F. N., A. M. Richter, A. K. Jain, J. G. Levy and C. Smits (1993) Biodistribution of a benzoporphyrin derivative-monooclonal antibody conjugate in A549-tumor-bearing nude mice. *Biotechnol. Ther.* **4**, 43–61.
 26. Molpus, K. L., M. R. Hamblin, I. Rizvi and T. Hasan (2000) Intraperitoneal photoimmunotherapy of ovarian carcinoma xenografts in nude mice using charged photoimmunocjugates. *Gynecol. Oncol.* **76**, 397–404.
 27. Pruss, R. M. and H. R. Herschman (1977) Variants of 3T3 cells lacking mitogenic response to epidermal growth factor. *Proc. Natl. Acad. Sci. USA* **74**, 3918–3921.
 28. Bodanszky, M. (1993) Side reactions due to overactivation. In *Principles of Peptide Synthesis*, 2nd revised ed., pp. 195, 196. Springer-Verlag, New York.
 29. Bauminger, S. and M. Wilchek (1980) The use of carbodiimides in the preparation of immunizing conjugates. *Methods Enzymol.* **70**, 151–159.
 30. Sambrook, J., E. F. Fritsch and T. Maniatis (1989) Spun-column chromatography. In *Molecular Cloning: A Laboratory Manual*, 2nd ed., pp. E.37, E.38. Cold Spring Harbor Laboratory Press, New York.
 31. Laemmli, U. K. (1970) Cleavage of structural proteins during the assembly of the head of bacteriophage T4. *Nature (Lond.)* **227**, 680–685.
 32. Hames, B. D. and D. Rickwood (eds.) (1996) *Gel Electrophoresis of Proteins: A Practical Approach*, pp. 46, 113–114. Oxford University Press Inc., New York.
 33. (1994) *TimeMaster Fluorescence Lifetime Spectrometer Reference Manual*. Photon Technology International, Inc., South Brunswick, NJ.
 34. (1998) *Fluorescence System User's Manual, Version 1.2x/TimeMaster Pro Software User's Manual*. Photon Technology International, Inc., Monmouth Junction, NJ.
 35. Bevington, P. R. (1969) *Data Reduction and Error Analysis for the Physical Sciences*. McGraw-Hill, New York.
 36. Mosmann, T. (1983) Rapid colorimetric assay for cellular growth and survival: application to proliferation and cytotoxicity assays. *J. Immunol. Methods* **65**, 55–63.
 37. Aveline, B. M., T. Hasan and R. W. Redmond (1995) The effects of aggregation, protein binding, and cellular incorporation on the photophysical properties of benzoporphyrin derivative monoacid ring A (BPDMA). *J. Photochem. Photobiol. B: Biol.* **30**, 161–169.
 38. Friedman, M. (1967) Solvent effects of amino groups in amino acids, peptides, and proteins with α , β -unsaturated compounds. *J. Am. Chem. Soc.* **89**, 4709–4713.
 39. Mew, D., C. K. Wat, C. K. Lum, G. H. N. Towers, C. H. C. Sun, R. T. Walter, M. W. Berns and J. G. Levy (1985) Ability of specific monoclonal antibodies and conventional antisera conjugated to hematoporphyrin to label and kill selected cell lines subsequent to light activation. *Cancer Res.* **45**, 4380–4386.
 40. Steele, K. J., D. Liu, A. T. Stammers, H. Deal, S. Whitney and J. G. Levy (1988) Suppressor deletion therapy: selective elimination of T suppressor cells using a hematoporphyrin conjugated monoclonal antibody. In *Antibody-mediated Delivery Systems*, pp. 157–189. Marcel Dekker, Inc., New York.
 41. Gross, S., A. Brandis, L. Chen, V. Rosenbach-Belkin, S. Roehrs, A. Scherz and Y. Salomon (1997) Protein-A-mediated targeting of bacteriochlorophyll-IgG to *Staphylococcus aureus*: a model for enhanced site-specific photocytotoxicity. *Photochem. Photobiol.* **66**, 872–878.
 42. Hamblin, M. R., J. L. Miller and B. Ortel (2000) Scavenger-receptor targeted photodynamic therapy. *Photochem. Photobiol.* **72**, 533–540.
 43. Suppan, P. (1994) *Chemistry and Light*, pp. 70–72. The Royal Society of Chemistry, Cambridge, UK.
 44. Goldstein, N. I., M. Prewett, K. Zuklys, P. Rockwell and J. Mendelsohn (1995) Biological efficacy of a chimeric antibody to the epidermal growth factor receptor in a human tumor xenograft model. *Clin. Cancer Res.* **1**, 1311–1318.
 45. Moan, J. (1986) Porphyrin photosensitization and phototherapy. *Photochem. Photobiol.* **43**, 681–690.
 46. Dougherty, T. J. (1996) A brief history of clinical photodynamic therapy development at Roswell Park Cancer Institute. *J. Clin. Laser Med.* **14**, 219–221.